

# Chapter 5

## Analysis of Effect of Solar Radiation Pressure of Bigger Primary on the Evolution of Periodic Orbits

In chapter 4 periodic orbits around both primaries –Sun–Mars and Sun–Earth systems– have been analyzed using PSS technique and the effects of oblateness of smaller primary on these orbits are analyzed. In this chapter we have analyzed effect of solar radiation pressure of bigger primary and actual oblateness of smaller primary on these orbits for the same systems. It is observed that solar radiation pressure of Sun has non–negligible effect on period and location of the orbit in the phase space. Also, geometrical parameters of the orbits like shape and size of the orbit are also affected due to this perturbation. In the design of low energy transfer trajectories this family of orbits can be used. So it is important to analyze this family of orbits under the effect of perturbations due to solar radiation pressure. It has been verified that stability of such orbits are negligible in comparison to family  $f$  orbits, so they can be used as transfer orbits. For each pair of solar radiation pressure  $q$  and Jacobi constant  $C$  we get two separatrices where stability of island becomes zero. Detailed stability analysis of periodic orbit with two–loops is done by taking  $q = 0.9845$ .

## 5.1 Introduction

A Hohmann transfer (Hohmann, 1925) is effectively used to transfer a spacecraft from one circular orbit to another in a most fuel efficient way. The low-energy transfer trajectory [Koon et. al.(2001)] is used to describe the space trajectories that consume less fuel compared to Hohman transfer (Hohmann, 1925). The planar restricted three body problem (PRTBP) has long been used in celestial mechanics and it is one of the simplest non-integrable dynamic systems.

The low-energy transfer orbits are important in the study of practical problems regarding transfer of orbits. Low energy transfer orbit to moon has been studied by [Koon et. al.(2001)]. In their study, they have considered four bodies Sun–Earth–Moon–Spacecraft as coupled three body systems, namely Sun–Earth–spacecraft and Earth–Moon–spacecraft. They have constructed low energy transfer trajectories from the Earth which executed capture at the Moon.

[Tsirogiannis et. al.(2006)] have studied Liapunov orbits in the photo-gravitational RTBP with oblateness. They have studied periodic motion around collinear equilibrium points for two and three dimensions. Using numerical analysis they have studied the effect of solar radiation pressure and oblateness on location and stability. [Perdiou et. al. (2012)] have computed periodic orbits of the Hill problem by considering solar radiation and oblateness as perturbing forces. [Elshaboury et. al. (2016)] have analyzed equilibrium points and periodic orbits of planar RTBP when both primaries are tri-axial rigid bodies. [Mittal et. al. (2009)] have studied periodic orbits generated by Lagrangian solutions of the RTBP when one of the primaries is an oblate body. [Mittal et. al.(2009)] have analyzed periodic orbits in the photo-gravitational restricted problem with the smaller primary as an oblate body. [Perdiou et. al. (2006)] have computed series of horizontally critical symmetric periodic orbits of the six basic families of the RTBP when the more massive primary is an oblate spheroid. The vertical stability of the horizontally critical orbits is also computed.

A large number of periodic orbits were generated by [Broucke (1968)] in the framework of RTBP numerically and classified the orbits into ten families. His work has been widely referred in literature. These studies explore the regions of the phase space that contain sensitive dependence on initial conditions. [Jefferys (1971)] and

[Contopoulos (1991)] have made extensive study on phase space by exploring large portion of the phase plane with PSS [Poincare (1892)]. This technique was also used by [Winter and Murray (1997a)] and [Winter and Murray (1997b)] to explore the phase space of a system with the Sun–Jupiter mass ratio.

In this chapter we have analyzed periodic orbits around both primaries with retrograde motion in rotating system and studied periodic orbits having number of loops from 1 to 5 for different pairs of solar radiation pressure  $q$  and Jacobi constant  $C$  for Sun–Mars and Sun–Earth systems. It has been found that  $q$  and  $C$  affect the position, shape and size of the orbits and hence must be considered during low energy trajectory design.

## 5.2 Results and discussion

In chapter 4 we have considered two systems, the Sun–Mars and Sun–Earth systems. For the Sun–Earth and Sun–Mars systems, mass factor  $\mu$  are taken as 0.000003002 and 0.0000003212, respectively. Oblateness coefficient for Sun–Earth and Sun–Mars have values  $A_2 = 2.42405 \times 10^{-12}$  and  $A_2 = 5.21389 \times 10^{-13}$  respectively.

For a given  $q$ , selection of  $C$  is not arbitrary. As described in earlier chapters using equation (1.4.21), admissible values of  $C$  have been obtained. Table 5.1 and Table 5.2 show the range of admissible values of  $C$  for Sun–Earth and Sun–Mars systems respectively. It can be observed that for Sun–Mars system size of excluded region is more than size of excluded region of Sun–Earth system. So, we can say that as mass factor increases, size of excluded region decreases. We have analyzed the effect of solar radiation pressure on admissible value of Jacobi constant  $C$ . We have studied the effect of solar radiation pressure on the location and period of Sun–Mars system for different values of  $C$  using PSS.

For simplicity in writing, the head rows of Table 5.1 and 5.2, solar radiation pressure, maximum value of  $C$ , value of  $C$  greater than maximum value of  $C$ , lower limit of excluded region, upper limit of excluded region and size of the excluded region are denoted by  $q$ ,  $C_M$ ,  $C$ ,  $LER$ ,  $UER$  and  $SER$ , respectively.

Equations (1.4.12) through (1.4.16) are equations of motion of secondary body in

Table 5.1: Admissible range of  $C$  for Sun–Earth system.

$q$	$C_M$	$C$	$LER$	$UER$	$SER$
1.0000	3.000	3.001	0.988	0.994	0.006
0.9950	2.990	2.991	0.985	0.994	0.009
0.9900	2.980	2.981	0.983	0.995	0.012
0.9845	2.969	2.970	0.980	0.995	0.015

Table 5.2: Admissible range of  $C$  for Sun–Mars system.

$q$	$C_M$	$C$	$LER$	$UER$	$SER$
1.0000	3.000	3.001	0.984	1.000	0.016
0.9950	2.990	2.991	0.982	1.000	0.018
0.9900	2.980	2.981	0.980	1.000	0.020
0.9845	2.969	2.970	0.978	0.995	0.022

the Sun–Mars and Sun–Earth system. Throughout this chapter value of  $A_2$  is taken as actual value of oblateness. In other words, effect of actual oblateness coefficient is taken into account. But  $q$  is taken as variable to know the effect of solar radiation pressure on this family of orbits.

Figure 5.1 depicts the PSS for Sun–Mars system for the pair  $(q, C) = (0.9845, 2.94)$  by taking value of  $x$  from the interval  $[0.8, 1]$  with interval of differences for  $x$  as 0.001. Also, time span  $t = 10,000$  time units and interval of differences for time is taken as 0.001. So, for each  $x$  equations of motions are integrated using Runge–Kutta–Gill method. Each solution is plotted as a point in the  $x-\dot{x}$  – plane as shown in Figure 5.1. The arcs of PSS are known as islands whose center gives periodic orbits.

In a similar way, we have obtained PSS for Sun–Earth system as shown in Figure 5.2. This PSS is also constructed for the pair  $(q, C)$  given by  $(0.9845, 2.94)$ . Our aim

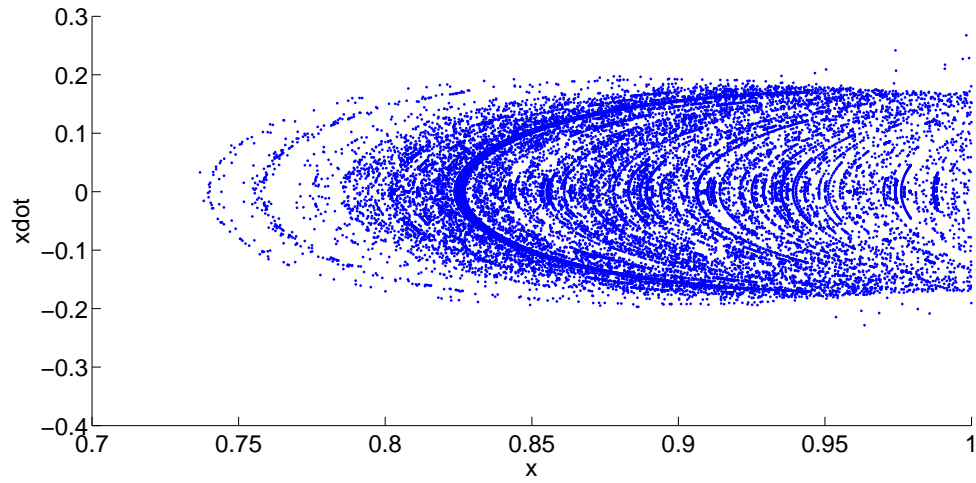


Figure 5.1: PSS for  $q = 0.9845$  and  $C = 2.94$ , for  $x = [0.8, 1]$  for Sun-Mars system.

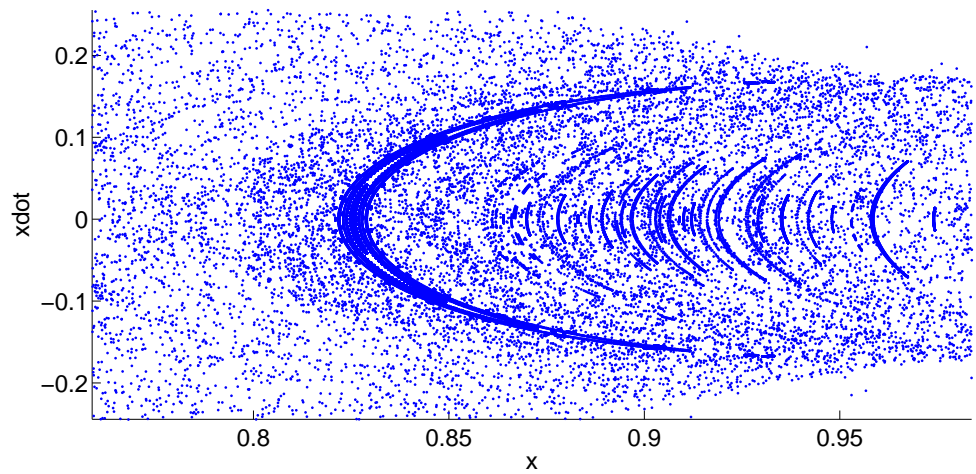
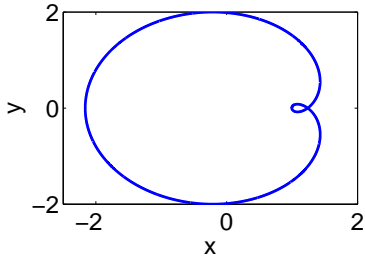


Figure 5.2: PSS for  $q = 0.9845$  and  $C = 2.94$ , for  $x = [0.8, 1]$  for Sun-Earth system.

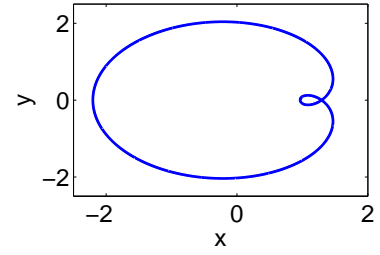
is to make a comparative study of the effect of solar radiation pressure on different parameters of the orbits of the secondary body (spacecraft) in the Sun–Earth and Sun–Mars systems using PSS technique.

The numerical values of location and period of periodic orbit of spacecraft for  $C = 2.94, 2.95, 2.96$  and for  $q = 1, 0.995, 0.99$  and  $0.9845$  are displayed in Table 5.3. It is observed from the table that a change in  $C$  from the the range  $(2.93, 2.96)$  affects the location but has no effect on the period and number of loops of the orbit. Solar radiation pressure also affects the location and period of the orbit. Similarly, the effects of  $C$  and  $q$  in the location and period for the Sun–Earth system are studied and the numerical estimates of the changes are displayed in Table 5.4. It can be seen that, for both the systems, the period of orbit increases with increase in the number of loops. A noticeable difference observed in both the systems is that, for Sun–Earth system, few orbits does not exist whereas they exist for Sun–Mars system. Single–loop orbit with  $(C = 2.96, q = 0.995)$ , two–loops orbit with  $(C = 2.96, q = 0.99)$  and three–loops orbit with  $(C = 2.96, q = 0.9845)$  does not exist for Sun–Earth system but they exists for Sun–Mars system.

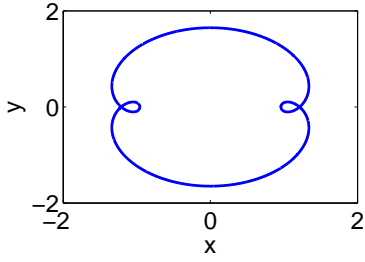
The periodic orbits starting from single–loop to five–loops in the Sun–Mars system for  $q = 0.9845$  and  $0.995$  are shown in Figures 5.3 (a)–(j). It can be observed, from Figure 5.3 and Figure 5.4, that the width of the orbit decreases continuously as the number of loops increases. Also, as perturbation due to solar radiation pressure decreases from  $q = 0.9845$  to  $0.995$ , the size of the loop increases. Further, it can be noticed that as the perturbation due to solar radiation pressure increases (that is,  $q$  decreases), the location of the closest approach of the spacecraft shifts towards the second primary body in both Sun–Mars and Sun–Earth systems. This is contrary to the effect of oblateness of the second primary. That is, as the oblateness coefficient increases the position of the closest approach of the spacecraft recedes from the second primary [Pathak and Thomas (2016c)]. Further, in all cases the secondary body (spacecraft) orbits around the second primary (Mars) in addition to orbiting both primaries. Further, the secondary body is closest to Mars in the single–loop closed orbit. Such orbits may be useful in the study of different aspects of both primaries. In many models available in literature not many closed orbits possess this kind of nature. We can observe similar nature in the orbits shown in Figures 5.4(a)–(j) in the case of Sun–Earth system.



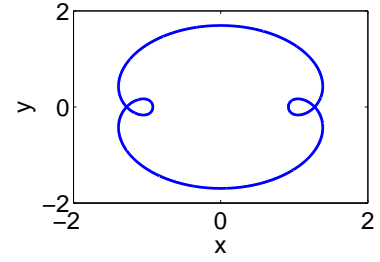
(a) Single-loop orbit for  $q = 0.9845$ .



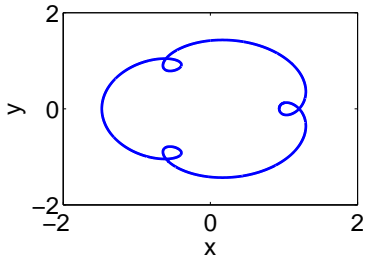
(b) Single-loop orbit for  $q = 0.995$ .



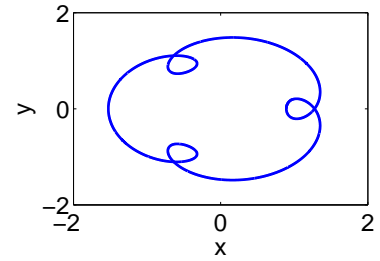
(c) Two-loops orbit for  $q = 0.9845$ .



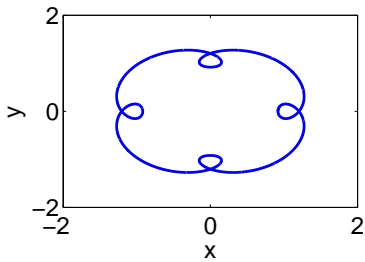
(d) Two-loops orbit for  $q = 0.995$ .



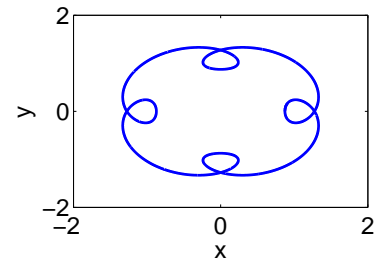
(e) Three-loops orbit for  $q = 0.9845$ .



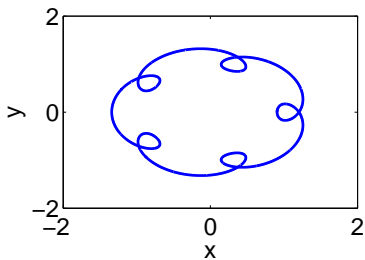
(f) Three-loops orbit for  $q = 0.995$ .



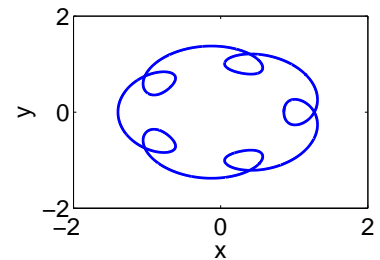
(g) Four-loops orbit for  $q = 0.9845$ .



(h) Four-loops orbit for  $q = 0.995$ .

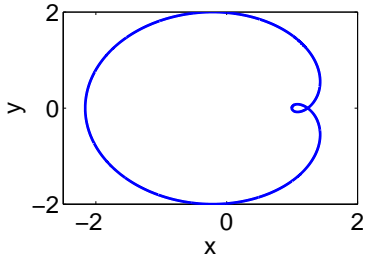


(i) Five-loops orbit for  $q = 0.9845$ .

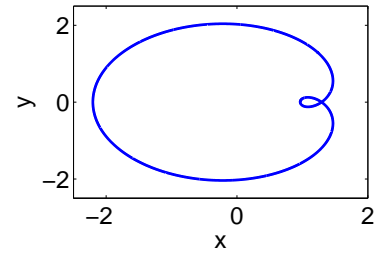


(j) Five-loops orbit for  $q = 0.995$ .

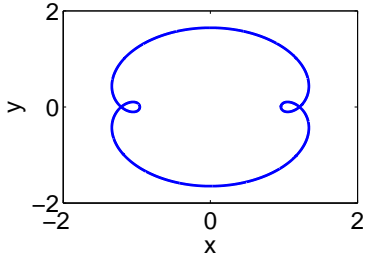
Figure 5.3: Periodic orbits around both primaries for Sun-Mars system when  $C = 2.94$ .



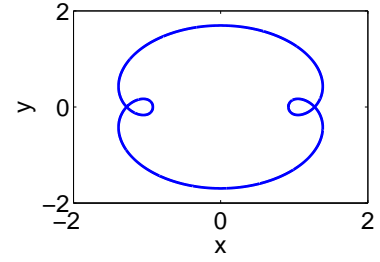
(a) Single-loop orbit for  $q = 0.9845$ .



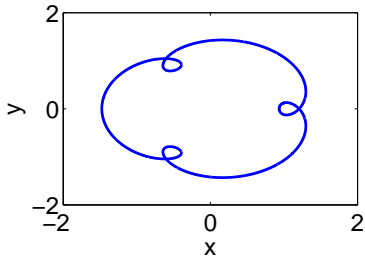
(b) Single-loop orbit for  $q = 0.995$ .



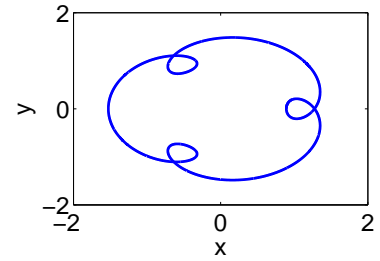
(c) Two-loops orbit for  $q = 0.9845$ .



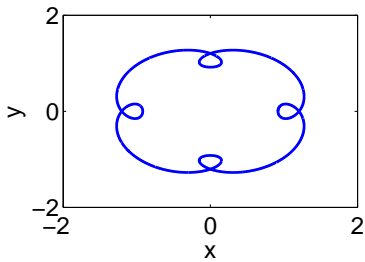
(d) Two-loops orbit for  $q = 0.995$ .



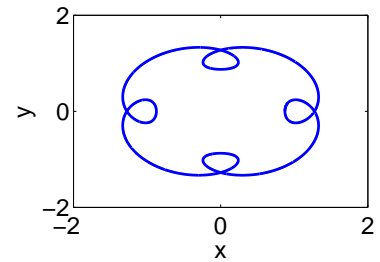
(e) Three-loops orbit for  $q = 0.9845$ .



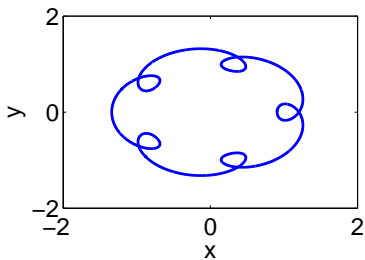
(f) Three-loops orbit for  $q = 0.995$ .



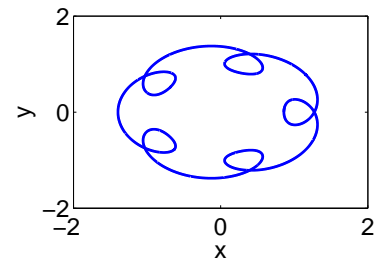
(g) Four-loops orbit for  $q = 0.9845$ .



(h) Four-loops orbit for  $q = 0.995$ .



(i) Five-loops orbit for  $q = 0.9845$ .



(j) Five-loops orbit for  $q = 0.995$ .

Figure 5.4: Periodic orbits around both primaries for Sun-Earth system when  $C = 2.94$ .

Figure 5.3 and Figure 5.4 depict periodic orbits with number of loops varying from 1 to 5 with different solar radiation pressure for Sun–Mars and Sun–Earth systems, respectively. For both of these figures  $C$  is 2.94.

Using the set of Equations (1.5.48) through (1.5.51), for different number of loops and selected values of  $C$  and  $q$ , the location of the orbit, the semi–major axis  $a$  and eccentricity  $e$  of the periodic orbits are calculated and numerical values are given for Sun–Mars system in Table 5.5.

From Table 5.5, it can be noticed that for a fixed number of loops, a decrease in the value of Jacobi constants from 2.96 to 2.93 cause the orbits to recede from Mars; the semi–major axis decreases and the eccentricity of the orbit increases. Similar effects can be observed for Sun–Earth system and the numerical estimates of these effects are displayed in Table 5.6.

We have studied the variation of position of periodic orbits around Sun–Mars and Sun–Earth systems due to variation in solar radiation pressure and Jacobi constants  $C$ . In Figure 5.5 we have shown the variation of position of closed periodic orbit with single–loop for solar radiation pressure in the range (0.9845, 1) for Sun–Mars system corresponding to  $C = 2.93$  and 2.94. From Figure 5.5 it is clear that the position of the orbits recedes from Mars when the solar radiation pressure decreases from 0.9845 to 1 and  $C$  decreases. Note that single–loop periodic orbits are not available for  $C = 2.95$  and 2.96. Similar kind of conclusion can be drawn from Figure 5.6 for the Sun–Earth system.

We have studied the effect of  $q$  and  $C$  on the position of the orbits having loops varying from 1 to 5 for both Sun–Mars and Sun–Earth systems. The results of these observations for five–loops closed periodic orbit in both Sun–Mars and Sun–Earth systems are shown in Figure 5.7 and Figure 5.8. From Figure 5.9 and Figure 5.10, it can be observed that for given solar radiation pressure, location of periodic orbit moves away from second primary as number of loops in periodic orbit increases. Also, as solar radiation pressure increases from 1 to 0.9845, location of periodic orbit moves towards second primary.

We have examined the effect of solar radiation pressure  $q$  for different values of Jacobi constants  $C$  on the semi–major axis of periodic orbits with single–loop and five–loops of Sun–Mars and Sun–Earth systems. The results of these effects are displayed in

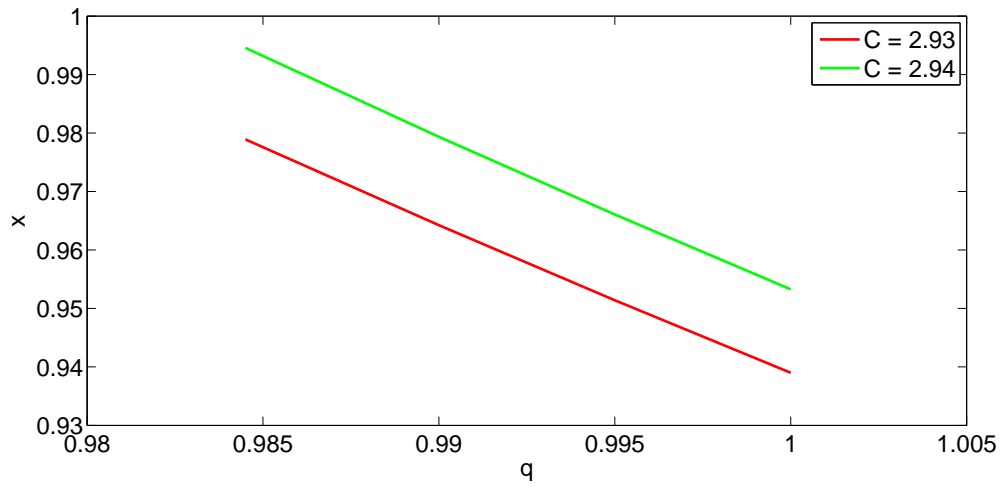


Figure 5.5: Variation in location of single-loop periodic orbit around Sun-Mars system due to solar radiation pressure.

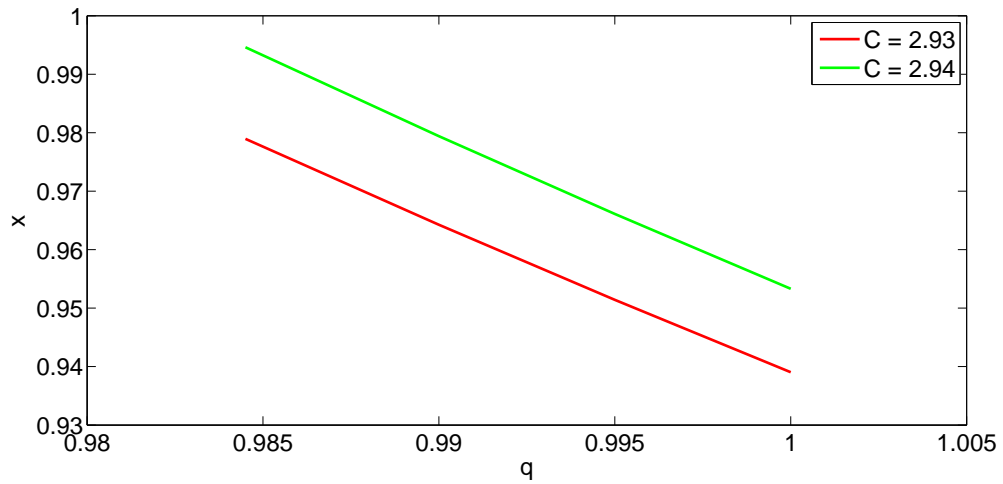


Figure 5.6: Variation in location of single-loop periodic orbit around Sun-Earth system due to solar radiation pressure.

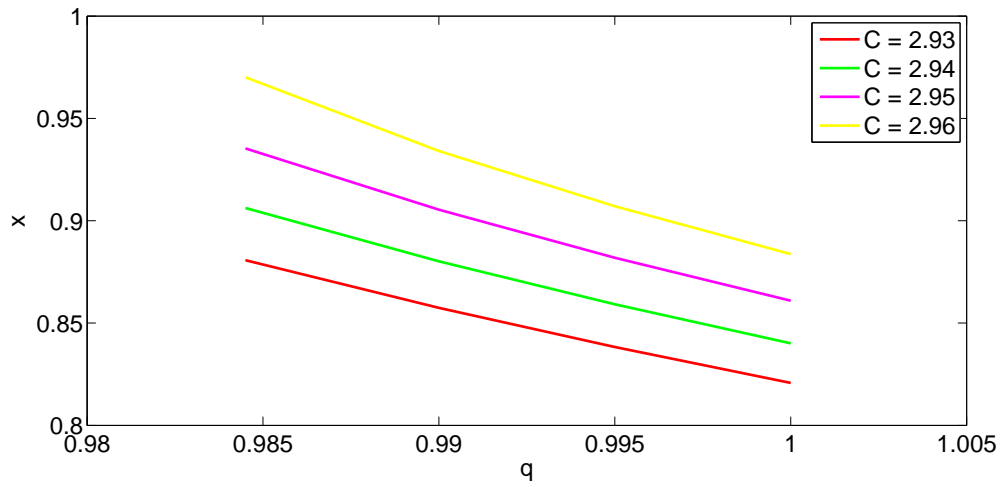


Figure 5.7: Variation in location of five-loops periodic orbit around Sun-Mars system due to solar radiation pressure.

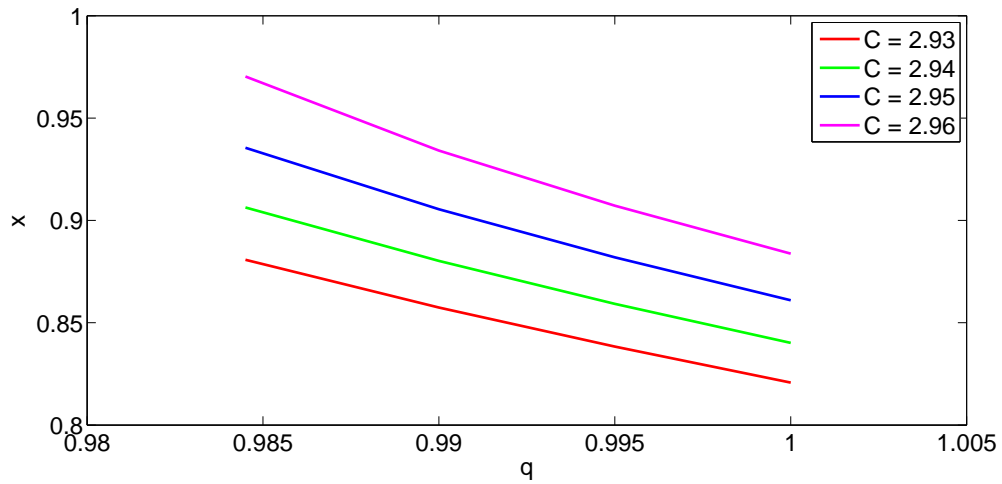


Figure 5.8: Variation in location of five-loops periodic orbit around Sun-Earth system due to solar radiation pressure.

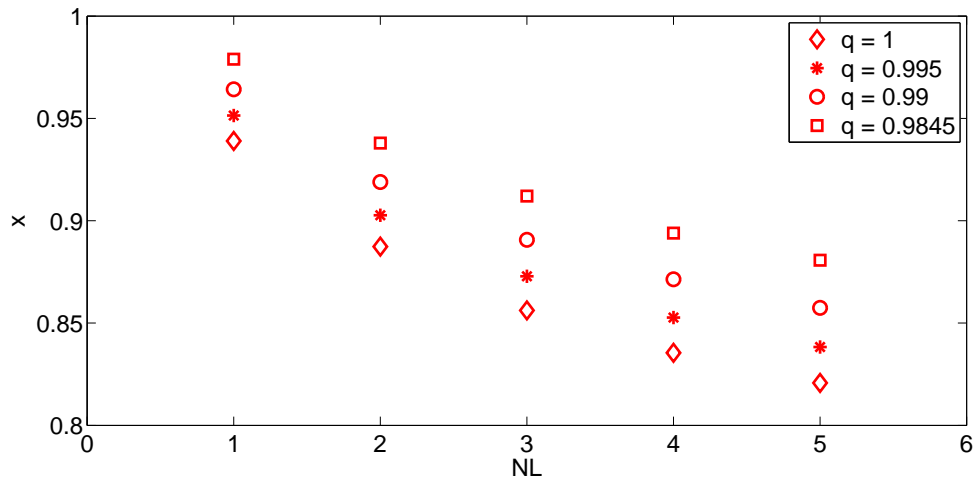


Figure 5.9: Variation in location of periodic orbit of secondary body around Sun and Mars for  $C = 2.93$  due to number of loops for different  $q$ .

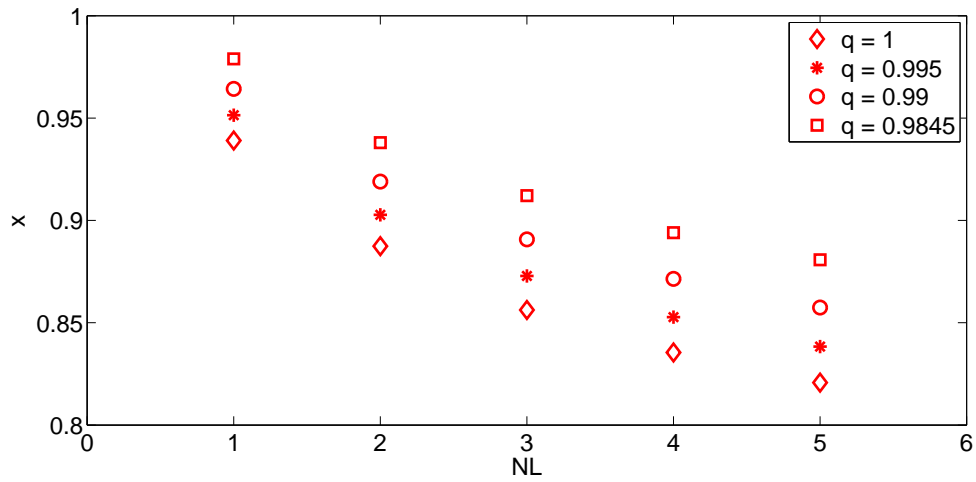


Figure 5.10: Variation in location of periodic orbit of secondary body around Sun and Earth for  $C = 2.93$  due to number of loops for different  $q$ .

Figures 5.11 through 5.14. While there are significant changes in the semi-major axis due to solar radiation pressure, the effect of  $C$  on the semi-major axis is less in comparison with that of  $q$ . Figures 5.11– 5.14 indicate that the semi-major axis decreases as solar radiation pressure increases from 1 to 0.9845. Figure 5.12 shows behavior of semi-major axis of single-loop periodic orbit for different solar radiation pressure. Green curve indicates variation of semi-major axis for  $C = 2.94$ . It shows non smooth behavior near  $q = 0.99$ , because single-loop periodic orbit for  $C = 2.94$  and  $q = 0.9845$  is located at  $x = 0.994601$  loose its periodicity after time  $t = 110$ . Figure 5.14 shows behavior of semi-major axis of five-loops periodic orbits for different  $q$ . Magenta curve indicates variation for semi-major axis for  $C = 2.96$ . It shows non smooth behavior near  $q = 0.99$ , because five-loops periodic orbit for  $C = 2.96$  and  $q = 0.9845$  is located at  $x = 0.9703$  loose its periodicity after time  $t = 500$ .

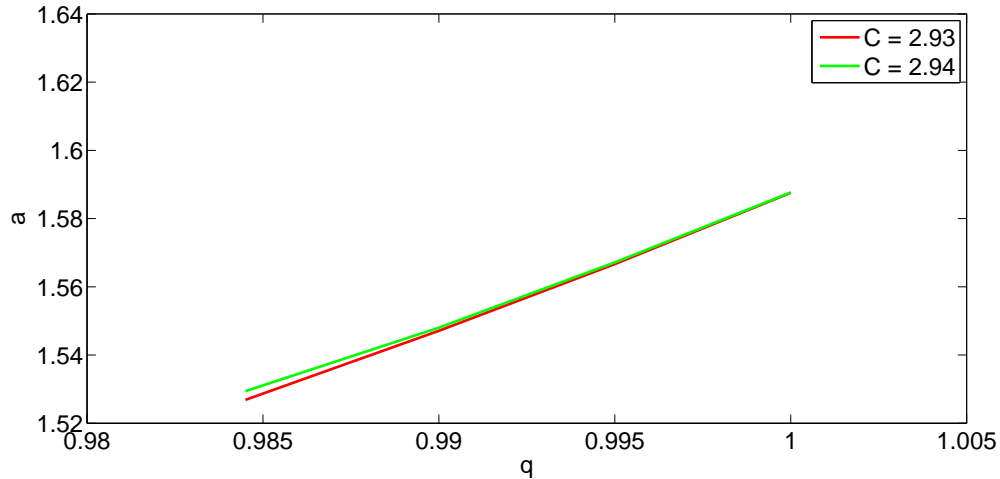


Figure 5.11: Variation in semi-major axis of single-loop periodic orbit around Sun–Mars system due to solar radiation pressure.

The variation of semi-major axis against the number of loops is examined for different solar radiation pressures and the results of the study are displayed in Figures 5.15 and 5.16. The semi-major axis decreases with increase in the number of loops. Further, for a fixed number of loops, the semi-major axis decreases with decrease in  $q$  from 1 to 0.9845.

From Figure 5.15 and Figure 5.16 it can be observed that, for given pair of  $C$  and  $q$ , as the number of loops increases semi-major axis decreases. Also, as  $q$  decreases from 1 to 0.9845 semi-major axis of periodic orbit for given number of loops decreases.

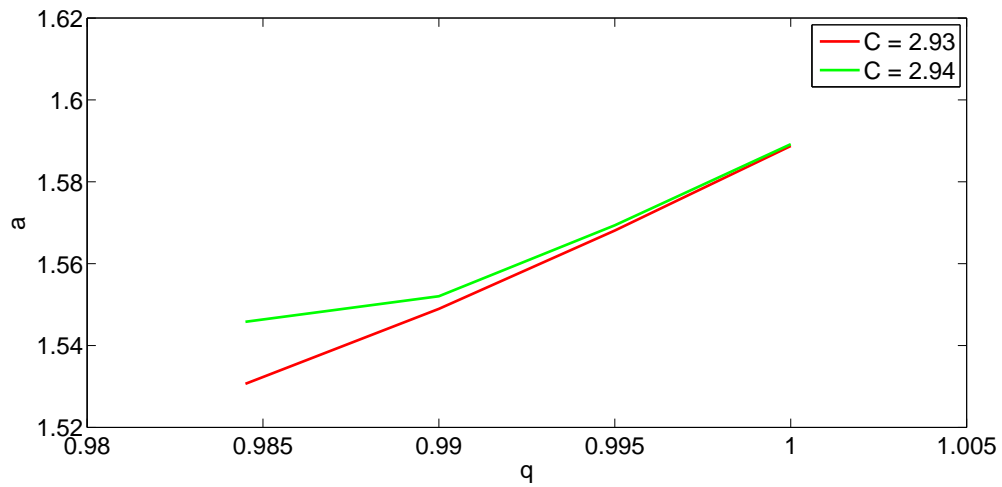


Figure 5.12: Variation in semi-major axis of single-loop periodic orbit around Sun-Earth system due to solar radiation pressure.

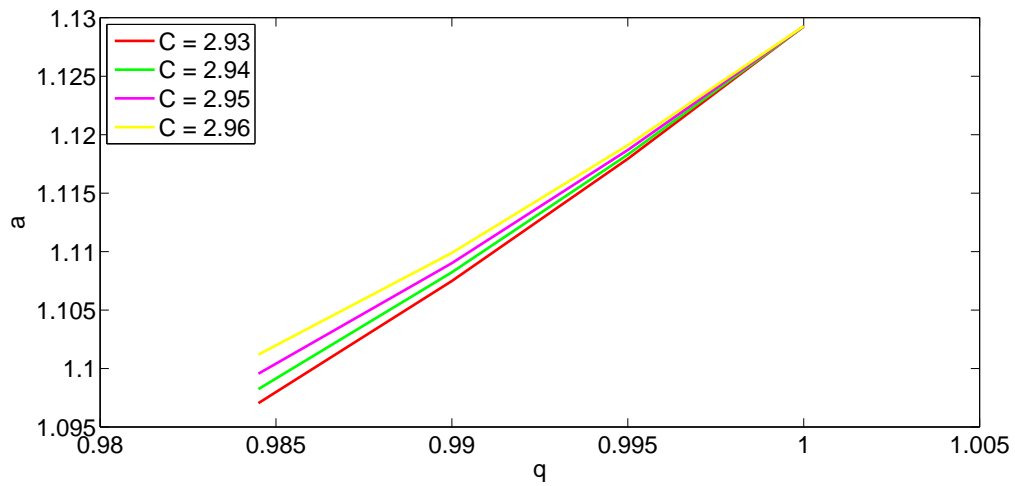


Figure 5.13: Variation in semi-major axis of five-loops periodic orbit around Sun-Mars system due to solar radiation pressure.

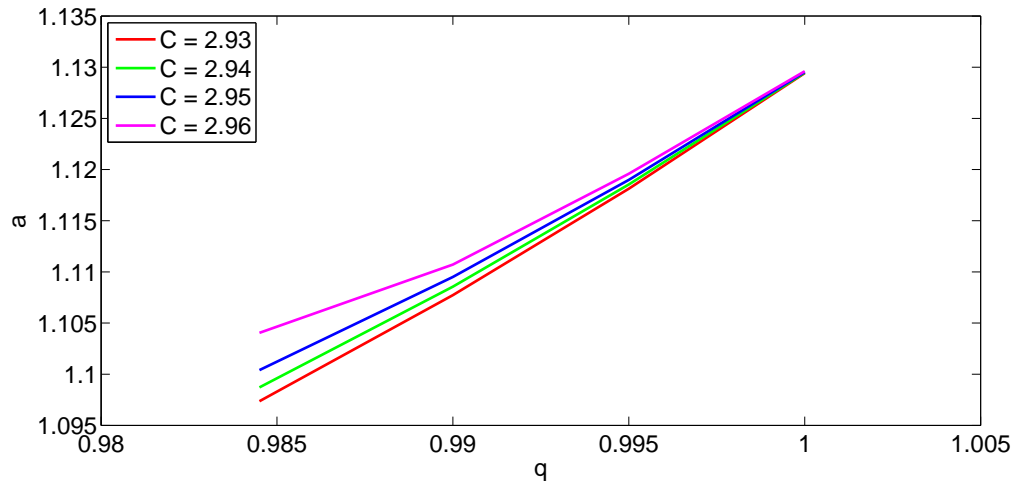


Figure 5.14: Variation in semi-major axis of five-loops periodic orbit around Sun-Earth system due to solar radiation pressure.

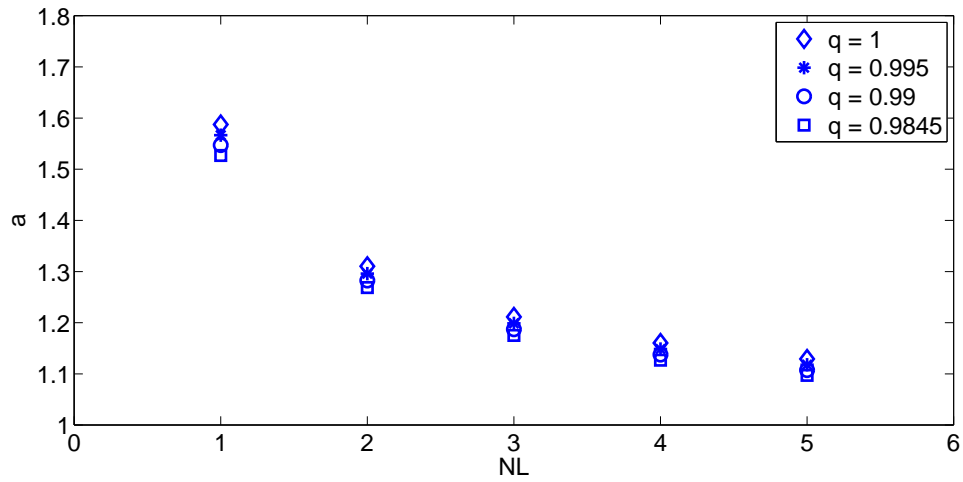


Figure 5.15: Variation in semi-major axis of periodic orbit of secondary body around Sun and Mars for  $C = 2.93$  due to number of loops for different  $q$ .

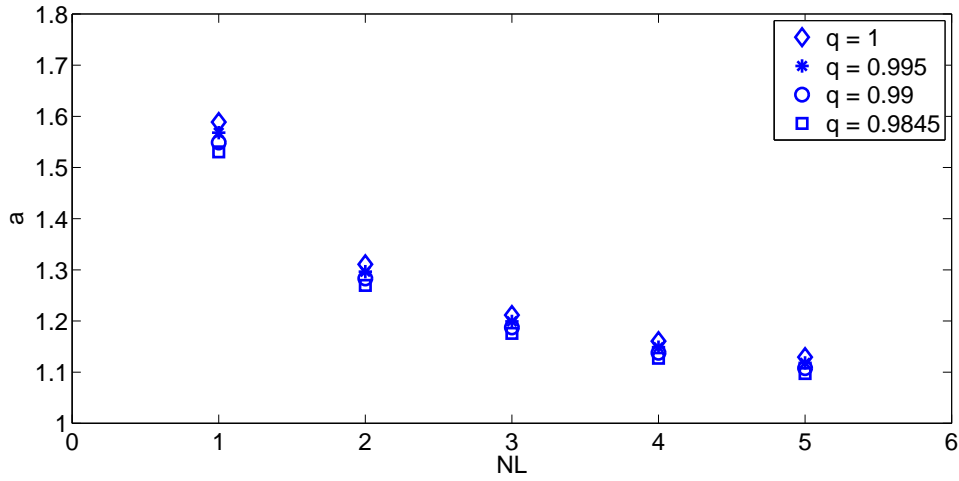


Figure 5.16: Variation in semi-major axis of periodic orbit of secondary body around Sun and Earth for  $C = 2.93$  due to number of loops for different  $q$ .

The variations of the other geometric parameter, viz, eccentricity  $e$  with respect to  $q$  and  $C$  for single and five-loops periodic orbits are shown in Figures 5.17 through 5.20 for both Sun–Mars and Sun–Earth systems. The eccentricity decreases as  $q$  decreases from 1 to 0.9845. Further, the eccentricity decreases as  $C$  increases for single-loop periodic orbit for both Sun–Mars and Sun–Earth systems as shown in Figures 5.17 and 5.18. Figure 5.18 shows variation in eccentricity of single-loop orbit corresponding to variation in  $q$  for given  $C$ . Green curve shows non smooth behavior corresponding to periodic orbit for  $C = 2.94$ ,  $q = 0.9845$  which is located at  $x = 0.994601$ , loose its periodicity after  $t = 110$ .

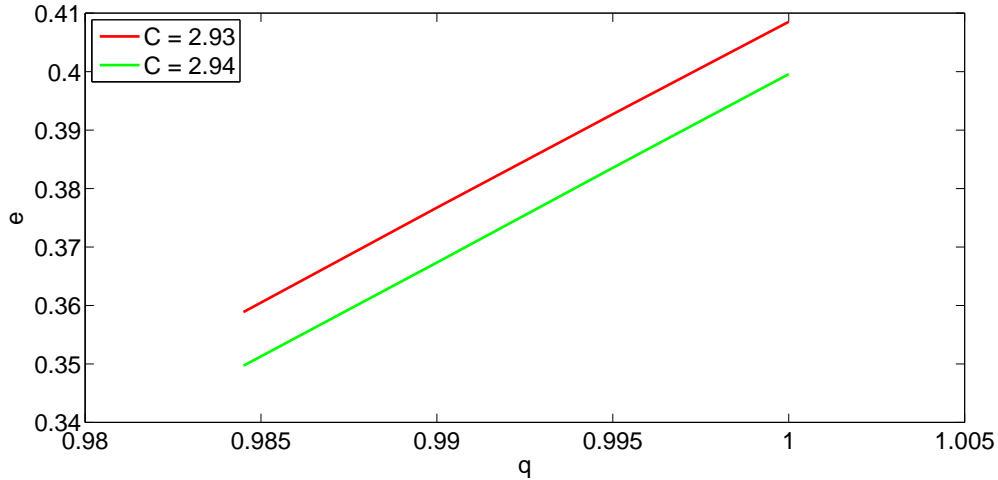


Figure 5.17: Variation in eccentricity of single-loop periodic orbit around Sun–Mars system due to solar radiation pressure.

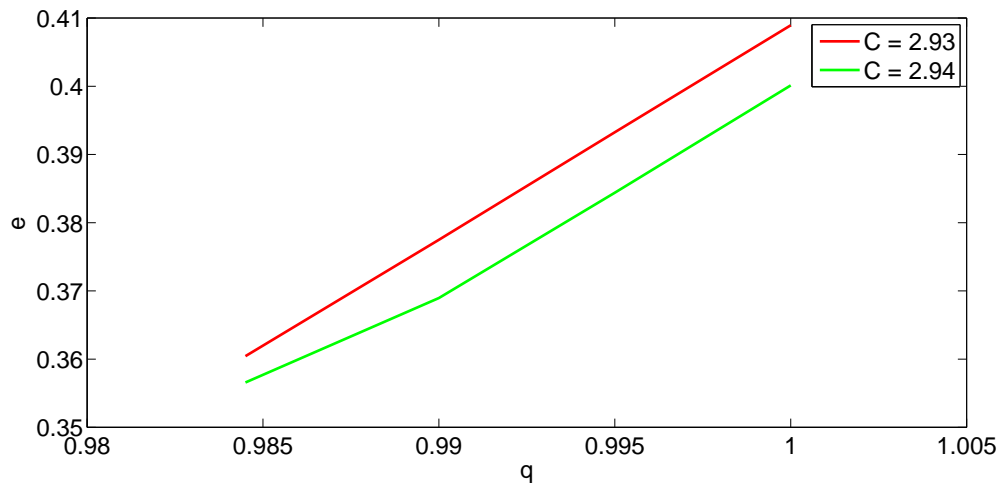


Figure 5.18: Variation in eccentricity of single-loop periodic orbit around Sun-Earth system due to solar radiation pressure.

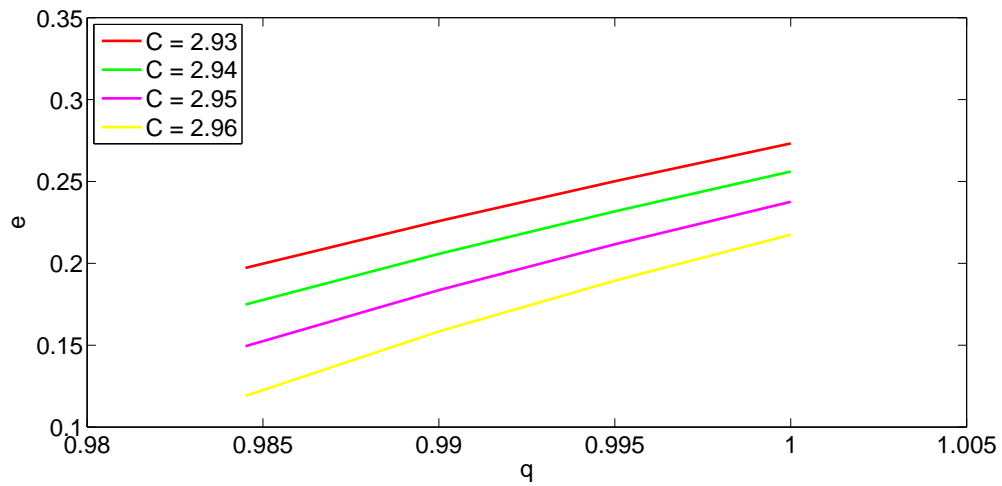


Figure 5.19: Variation in eccentricity of five-loops periodic orbit around Sun-Mars system due to solar radiation pressure.

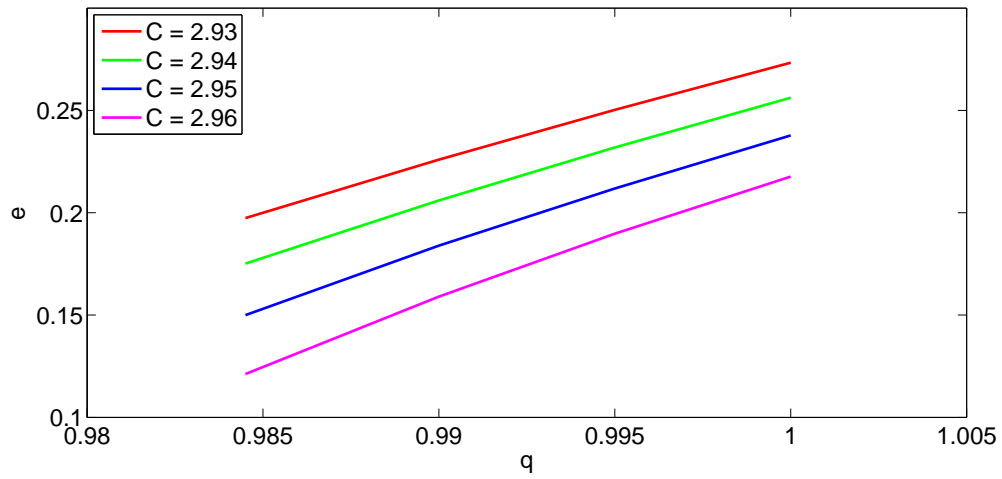


Figure 5.20: Variation in eccentricity of five-loops periodic orbit around Sun–Earth system due to solar radiation pressure.

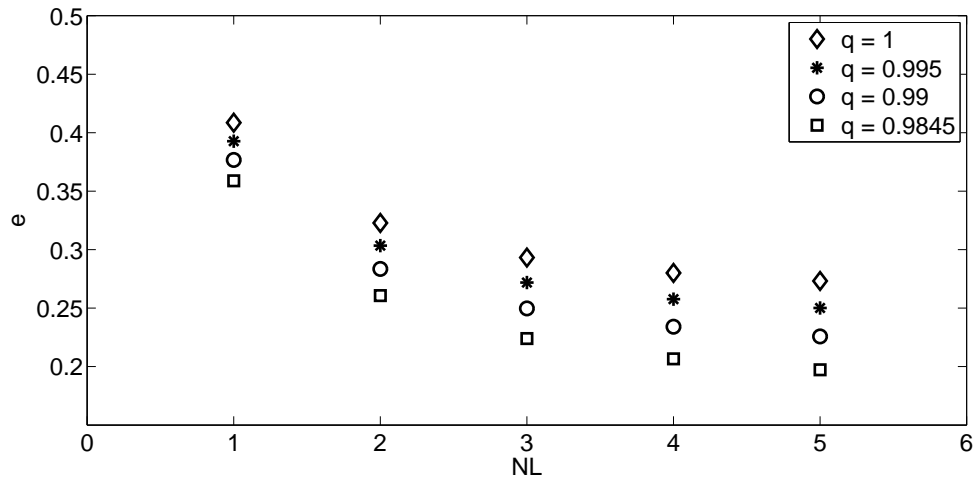


Figure 5.21: Variation in eccentricity of periodic orbit of secondary body around Sun and Mars for  $C = 2.93$  due to number of loops for different  $q$ .

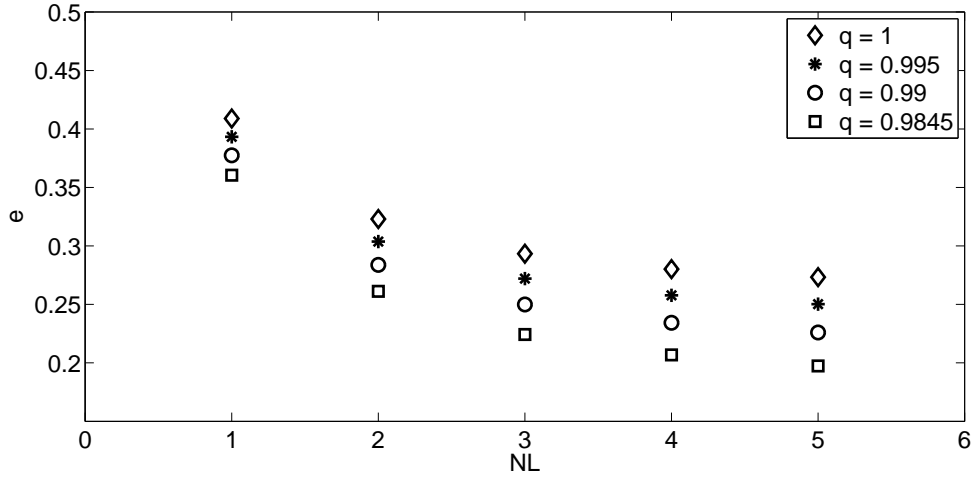


Figure 5.22: Variation in eccentricity of periodic orbit of secondary body around Sun and Earth for  $C = 2.93$  due to number of loops for different  $q$ .

We have also analyzed the effect of number of loops on the eccentricity of the orbit. These effects are depicted in Figures 5.21 and 5.22. It is found that the eccentricity decreases as number of loops increases. For a given loop, eccentricity decreases as  $q$  decreases from 1 to 0.9845.

In Table 5.5 initial velocity of secondary body is denoted by  $V$ ,  $D_1$  and  $D_2$  are the distance of secondary body from Mars and Sun respectively.  $V$  is measured in  $km.s^{-1}$ ,  $D_1$  and  $D_2$  are in kms. Similar notations are used in Table 5.6 also. In Table 5.6 distance of secondary body from Earth is denoted by  $D_1$  and  $V$  is calculated by using

$$V = \sqrt{\dot{x}^2 + [\dot{y} + n(x + \mu)]^2}. \quad (5.2.1)$$

The conversion from units of distance ( $I$ ) and velocity ( $J$ ) in the normalized dimensionless system to the dimensionalized system is given by,

$$D = R \times I, \quad (5.2.2)$$

$$V = O \times J \quad (5.2.3)$$

where  $R$  is the distance between the centers of both primaries in km.  $O$  is the orbital velocity of second primary around first primary [Koon et. al.(2011)]. For Sun–Mars and Sun–Earth system  $R = 227,940,000$  kms and  $149,600,000$  kms respectively. Mean orbital velocity of Mars around Sun and Earth around Sun are  $24.07 km.s^{-1}$  and  $29.78 km.s^{-1}$  respectively.

It can be observed from Tables 5.7 and 5.8 that for given solar radiation pressure and given number of loops, as  $C$  decreases,  $V$  and  $D_1$  increase while  $D_2$  decreases. For a given  $C$  and given number of loops, as  $q$  decreases from 1 to 0.9845, initial velocity  $V$  and  $D_1$  decrease and,  $D_2$  increases. So, the effect of  $C$  and solar radiation pressure  $q$  is opposite in nature. For given value of  $q$  and  $C$  as number of loops increases,  $D_1$  increases and  $D_2$  decreases.

From Table 5.7, it is observed that single-loop orbit for  $q = 1$  is closest to Mars and this distance is  $7.521 \times 10^7$  kms. which is obtained by taking the values of  $C = 2.96$  and  $q = 0.995$ . From Table 5.8, it is observed that single-loop orbit for  $q = 0.99$  is closest to Earth and this distance is  $7.535 \times 10^5$  km. This orbit is obtained by taking  $C = 2.95$ .

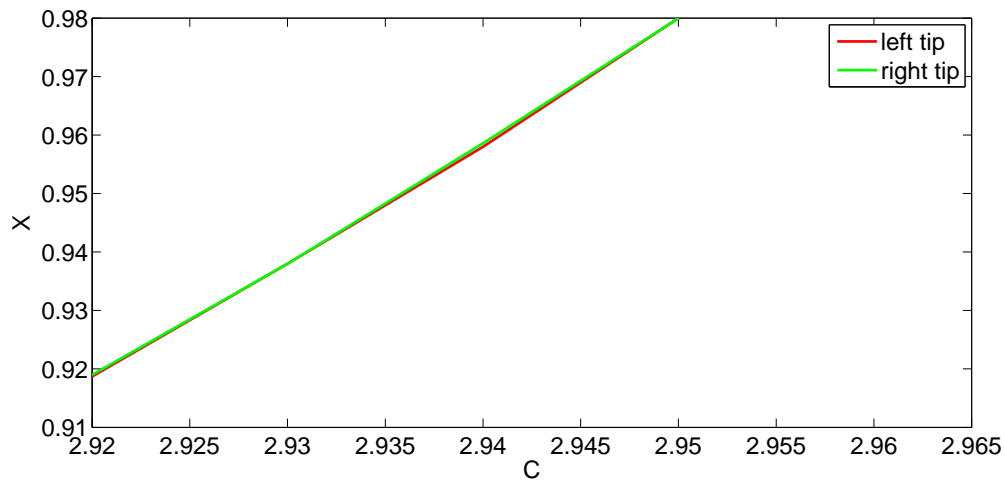


Figure 5.23: Stability analysis for two-loops orbit for Sun-Earth system when  $q = 0.9845$ .

We have analyzed stability of periodic orbits from loop 1 to 5 for  $q = 1, 0.995, 0.99$  and  $0.9845$ . Since stability behavior is similar for all these orbits, stability analysis for two-loops orbit corresponding to  $q = 0.9845$  is given. Figure 5.23 shows stability region for  $q = 0.9845$  for two-loops orbit. The left and right tips of the island are plotted by red and green curves, respectively. From Figure 5.23, it is clear that size of stability region is very small in comparison to  $f$  family orbit [Pathak and Thomas(2016b)]. So, these periodic orbits can be used as transfer orbits as they are not stable. So, secondary body in this case required few amount of fuel for transfer using this orbit in comparison of Hohmann transfer. Figure 5.24 shows amplitude for two-loops orbit when  $q = 0.9845$ . It can be observed that there are

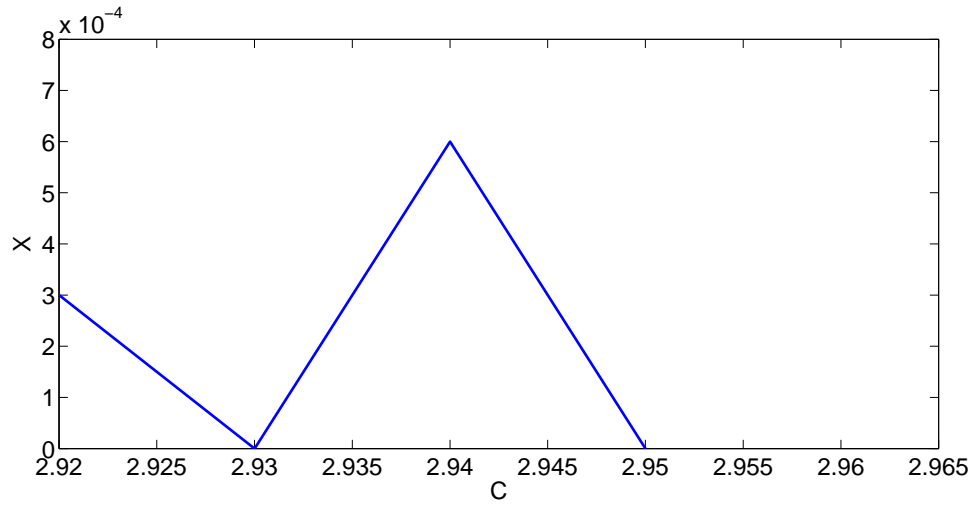


Figure 5.24: Amplitude for two-loops orbit for Sun-Earth system when  $q = 0.9845$ .

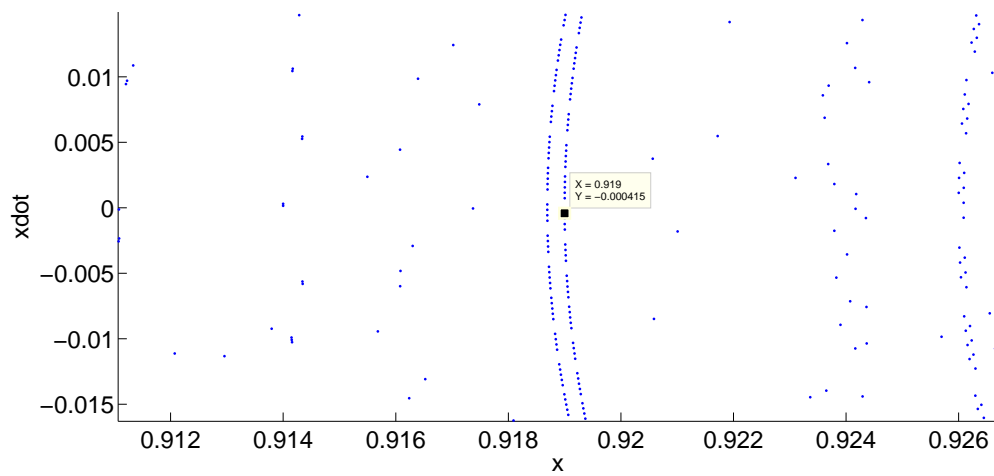


Figure 5.25: Enlarge view of PSS for  $C = 2.92$  when  $q = 0.9845$ .

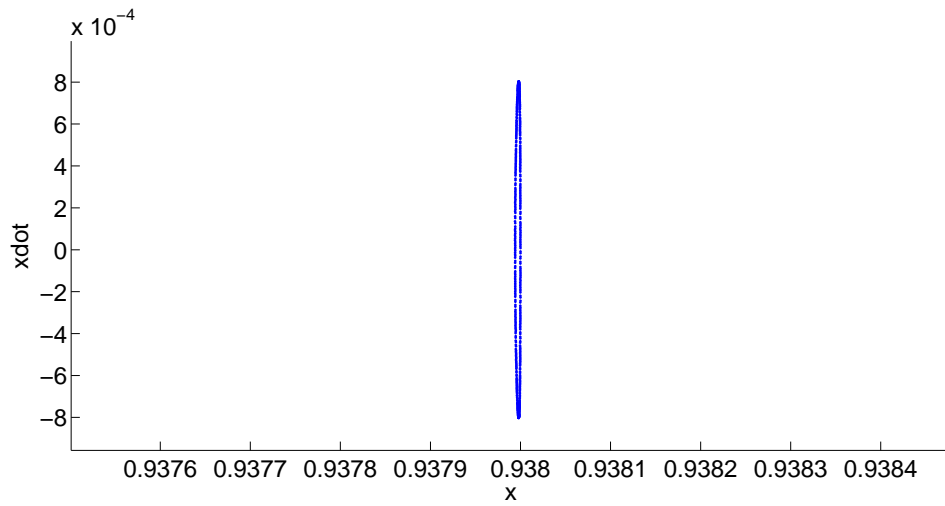


Figure 5.26: Enlarge view of PSS of first separatrix for two-loops orbit for  $C = 2.93$  when  $q = 0.9845$ .

two separatrices at  $C = 2.93$  and  $2.95$  where stability of the periodic orbit is zero as the size of the island is zero. For  $C = 2.94$  we get maximum stability. Size of the largest island is  $0.0006$ . Figure 5.25 shows size of the island for  $C = 2.92$  for two-loops orbit when  $q = 0.9845$  which is  $0.0003$ . Figure 5.26 shows PSS of first separatrix at  $C = 2.93$  which looks like a straight line whereas for  $f$  family orbit it is triangular due to third order resonance [Pathak and Thomas(2016b)]. It can be seen that size of this island is zero. Figure 5.27 shows two-loops orbit corresponding to first separatrix when  $q = 0.9845$ . Figure 5.28 shows for  $C = 2.94$  again size of island increases and it becomes maximum. For  $C = 2.95$  size of island becomes zero, which is second separatrix as shown in Figure 5.29. Two-loops orbit corresponding to second separatrix is given in Figure 5.30.

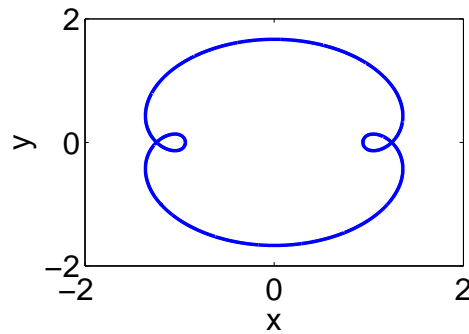


Figure 5.27: Orbit at first separatrix corresponding to  $C = 2.93$ ,  $q = 0.9845$  and  $x = 0.938$ .

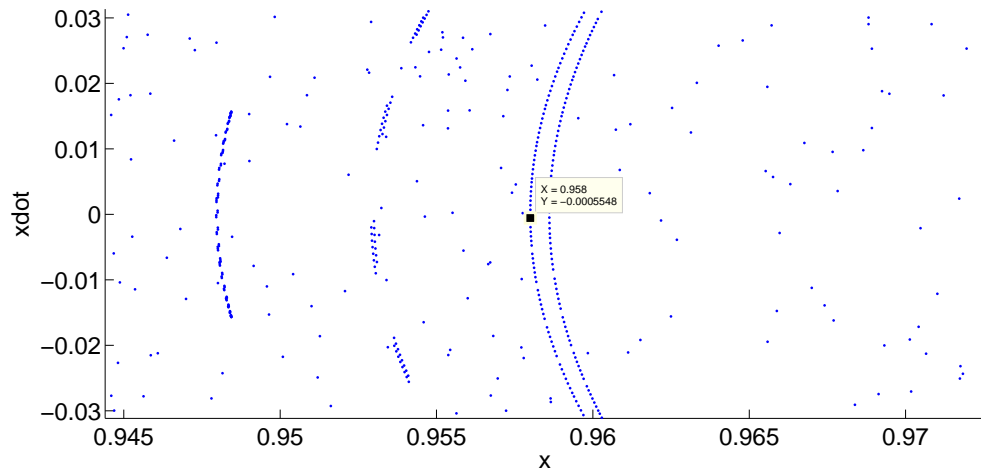


Figure 5.28: Enlarge view of PSS for  $C = 2.94$  when  $q = 0.9845$ .

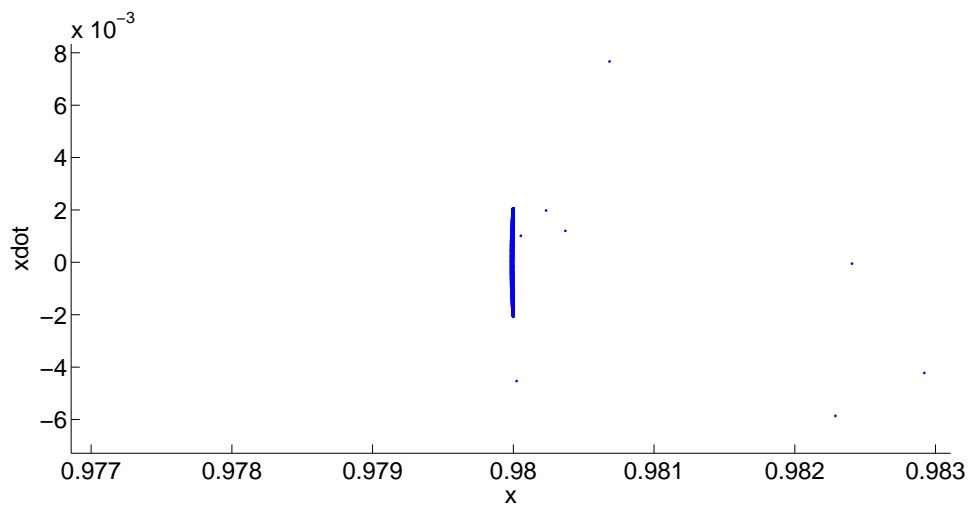


Figure 5.29: Enlarge view of PSS of second separatrix for two-loops orbit for  $C = 2.95$ ,  $q = 0.9845$ .

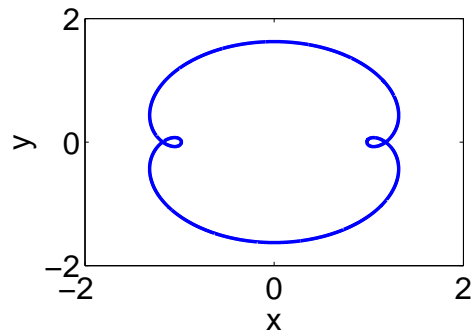


Figure 5.30: Orbit at second separatrix corresponding to  $C = 2.95$ ,  $q = 0.9845$ , and  $x = 0.98$ .

Table 5.3: Analysis of periodic orbit for different pairs of  $q$  and  $C$  for Sun–Mars system.

$NL$	$C$	$q = 1$		$q = 0.995$		$q = 0.99$		$q = 0.9845$	
		$x$	$T$	$x$	$T$	$x$	$T$	$x$	$T$
1	2.96	0.983000	13	0.996700	13	-	-	-	-
	2.95	0.967910	13	0.981150	13	0.994900	13	-	-
	2.94	0.953270	13	0.966070	13	0.979350	13	0.99455	13
	2.93	0.939000	13	0.951390	13	0.964240	13	0.97891	13
2	2.96	0.941520	19	0.959850	19	0.979570	19	-	-
	2.95	0.922550	19	0.939710	19	0.958070	19	0.97992	19
	2.94	0.904540	19	0.920710	19	0.937920	19	0.95825	19
	2.93	0.887370	19	0.902690	19	0.918910	19	0.93795	19
3	2.96	0.915320	26	0.936300	26	0.959570	26	0.98875	26
	2.95	0.894290	26	0.913530	26	0.934550	26	0.96036	26
	2.94	0.874650	26	0.892480	26	0.911750	26	0.93506	26
	2.93	0.856190	26	0.872830	26	0.890690	26	0.91204	26
4	2.96	0.897070	32	0.919590	32	0.945100	32	0.97830	32
	2.95	0.874940	32	0.895290	32	0.917850	32	0.94620	32
	2.94	0.854500	32	0.873140	32	0.893530	32	0.91857	32
	2.93	0.835433	32	0.852695	32	0.871375	32	0.89397	32
5	2.96	0.883675	38	0.907110	38	0.934050	38	0.97010	38
	2.95	0.860930	38	0.881900	38	0.905380	38	0.93535	38
	2.94	0.840070	38	0.859150	38	0.880160	38	0.90623	38
	2.93	0.820715	38	0.838290	38	0.857400	38	0.88069	38

Table 5.4: Analysis of periodic orbit for different pairs of  $q$  and  $C$  for Sun–Earth system.

$NL$	$C$	$q = 1$		$q = 0.995$		$q = 0.99$		$q = 0.9845$	
		$x$	$T$	$x$	$T$	$x$	$T$	$x$	$T$
1	2.96	0.98305	13	-	-	-	-	-	-
	2.95	0.96795	13	0.98120	13	0.99496	13	-	-
	2.94	0.95330	13	0.96610	13	0.97940	13	0.99460	13
	2.93	0.93904	13	0.95142	13	0.96425	13	0.97895	13
2	2.96	0.94157	19	0.95990	19	-	-	-	-
	2.95	0.92259	19	0.93975	19	0.95813	19	0.98000	19
	2.94	0.90456	19	0.92075	19	0.93796	19	0.95830	19
	2.93	0.88740	19	0.90273	19	0.91895	19	0.93800	19
3	2.96	0.91538	26	0.93635	26	0.95965	26	-	-
	2.95	0.89434	26	0.91359	26	0.93462	26	0.96045	26
	2.94	0.87469	26	0.89252	26	0.91181	26	0.93513	26
	2.93	0.85623	26	0.87287	26	0.89074	26	0.91210	26
4	2.96	0.89714	32	0.91965	32	0.94520	32	0.97844	32
	2.95	0.87499	32	0.89535	32	0.91793	32	0.94630	32
	2.94	0.85454	32	0.87320	32	0.89359	32	0.91865	32
	2.93	0.83547	32	0.85274	32	0.87142	32	0.89403	32
5	2.96	0.88373	38	0.90719	38	0.93415	38	0.97030	38
	2.95	0.86099	38	0.88195	38	0.90546	38	0.93547	38
	2.94	0.84012	38	0.85920	38	0.88022	38	0.90630	38
	2.93	0.82075	38	0.83833	38	0.85745	38	0.88075	38

Table 5.5: Location, semi major axis and eccentricity of orbits for  $q = 1, 0.995, 0.99$  and  $0.9845$  for Sun–Mars system.

$NL$	$C$	$q = 1$			$q = 0.995$			$q = 0.99$			$q = 0.9845$		
		$x$	$a$	$e$	$x$	$a$	$e$	$x$	$a$	$e$	$x$	$a$	$e$
1	2.96	0.983000	1.5880	0.3809	0.996700	1.5707	0.3654	-	-	-	-	-	-
	2.95	0.967910	1.5876	0.3903	0.981150	1.5676	0.3741	0.994900	1.5501	0.3581	-	-	-
	2.94	0.953270	1.5876	0.3995	0.966070	1.5671	0.3835	0.979350	1.5480	0.3673	0.994550	1.5294	0.3497
	2.93	0.939000	1.5875	0.4085	0.951390	1.5666	0.3927	0.964240	1.5470	0.3767	0.978910	1.5268	0.3588
2	2.96	0.941520	1.3104	0.2815	0.959850	1.2972	0.2600	0.979570	1.2850	0.2377	-	-	-
	2.95	0.922550	1.3104	0.29601	0.939710	1.2967	0.2753	0.958070	1.2840	0.2538	0.979920	1.2713	0.2292
	2.94	0.904540	1.3104	0.3097	0.920710	1.2963	0.2897	0.937920	1.2831	0.2690	0.958250	1.2699	0.2454
	2.93	0.887370	1.3104	0.3228	0.902690	1.2959	0.3034	0.918910	1.2824	0.2834	0.937950	1.2686	0.2606
3	2.96	0.915320	1.2114	0.2444	0.936300	1.1999	0.2197	0.959570	1.1895	0.1933	0.988750	1.1798	0.1619
	2.95	0.894290	1.2114	0.2618	0.913530	1.1995	0.2384	0.934550	1.1886	0.2137	0.960360	1.1777	0.1845
	2.94	0.874650	1.2114	0.2780	0.892480	1.1991	0.2557	0.911750	1.1878	0.2324	0.935060	1.1764	0.2051
	2.93	0.856190	1.2114	0.2932	0.872830	1.1988	0.2719	0.890690	1.1871	0.2496	0.912040	1.1752	0.2239
4	2.96	0.897070	1.1604	0.2269	0.919590	1.1497	0.2002	0.945100	1.1401	0.1710	0.978300	1.1311	0.1351
	2.95	0.874940	1.1604	0.2460	0.895290	1.1492	0.2210	0.917850	1.1392	0.1943	0.946200	1.1293	0.1621
	2.94	0.854500	1.1604	0.2636	0.873140	1.1489	0.2400	0.893530	1.1384	0.2151	0.918570	1.1279	0.1856
	2.93	0.835433	1.1604	0.2800	0.852695	1.1486	0.2576	0.871375	1.1377	0.2341	0.893970	1.1267	0.2066
5	2.96	0.883675	1.1292	0.2174	0.907110	1.1191	0.1894	0.934050	1.1099	0.1584	0.970100	1.1012	0.1190
	2.95	0.860930	1.1292	0.2376	0.881900	1.1186	0.2116	0.905380	1.1090	0.1836	0.935350	1.0995	0.1493
	2.94	0.840070	1.1292	0.2560	0.859150	1.1183	0.2317	0.880160	1.1082	0.2058	0.906230	1.0982	0.1748
	2.93	0.820715	1.1292	0.2732	0.838290	1.1179	0.2501	0.857400	1.1074	0.2258	0.880690	1.0970	0.1972

Table 5.6: Location, semi major axis and eccentricity of orbits for  $q = 1, 0.995, 0.99$  and  $0.9845$  for Sun–Earth system.

$NL$	$C$	$q = 1$			$q = 0.995$			$q = 0.99$			$q = 0.9845$		
		$x$	$a$	$e$	$x$	$a$	$e$	$x$	$a$	$e$	$x$	$a$	$e$
1	2.96	0.9830	1.5931	0.38293	-	-	-	-	-	-	-	-	-
	2.95	0.96795	1.5900	0.3912	0.98120	1.5721	0.3758	0.99496	1.5680	0.3654	-	-	-
	2.94	0.95330	1.5891	0.4001	0.96610	1.5693	0.3844	0.97940	1.5520	0.3689	0.994601	1.5458	0.3565
	2.93	0.93904	1.5887	0.4089	0.95142	1.5680	0.3932	0.96425	1.5489	0.3774	0.97895	1.5306	0.3604
2	2.96	0.94157	1.3114	0.2820	0.95990	1.2988	0.2609	-	-	-	-	-	-
	2.95	0.92259	1.3111	0.2963	0.93975	1.2976	0.2757	0.95813	1.2855	0.2546	0.9800	1.2751	0.2314
	2.94	0.90456	1.3108	0.3099	0.92075	1.2969	0.2900	0.93796	1.2840	0.2695	0.95830	1.2713	0.2462
	2.93	0.88740	1.3108	0.3230	0.90273	1.2964	0.3036	0.91895	1.2830	0.2837	0.93800	1.2695	0.2611
3	2.96	0.91538	1.2120	0.2447	0.93635	1.2007	0.2202	0.95965	1.1911	0.1943	-	-	-
	2.95	0.89434	1.2118	0.2620	0.91359	1.2001	0.2387	0.93462	1.1894	0.2142	0.96045	1.1794	0.1856
	2.94	0.87469	1.2117	0.2781	0.89252	1.1995	0.2559	0.91181	1.1883	0.2327	0.93513	1.1772	0.2057
	2.93	0.85623	1.2117	0.2933	0.87287	1.1991	0.2720	0.89074	1.1874	0.2499	0.91210	1.1758	0.2242
4	2.96	0.89714	1.1608	0.2272	0.91965	1.1503	0.2005	0.94520	1.1412	0.1717	0.97844	1.1350	0.1380
	2.95	0.87499	1.1607	0.2461	0.89535	1.1498	0.2213	0.91793	1.1398	0.1947	0.94630	1.1304	0.1628
	2.94	0.85454	1.1606	0.2637	0.87320	1.1493	0.2402	0.89359	1.1388	0.2153	0.91865	1.1285	0.1860
	2.93	0.83547	1.1606	0.2801	0.85274	1.1488	0.2577	0.87142	1.1380	0.2342	0.89403	1.1271	0.2068
5	2.96	0.88373	1.1296	0.2176	0.90719	1.1195	0.1897	0.93415	1.1107	0.1589	0.97030	1.1040	0.1211
	2.95	0.86099	1.1295	0.2377	0.88195	1.1189	0.2118	0.90546	1.1095	0.1839	0.93547	1.1004	0.1499
	2.94	0.84012	1.1294	0.2561	0.85920	1.1185	0.2318	0.88022	1.1085	0.2059	0.90630	1.0987	0.1751
	2.93	0.82075	1.1294	0.2733	0.83833	1.1181	0.2502	0.85745	1.1077	0.2259	0.88075	1.0973	0.1974

Table 5.7: Location, velocity and distance of orbit from both primaries for  $q = 1, 0.995, 0.99, 0.9845$  for Sun–Mars system.

$NL$	$C$	$q = 1$				$q = 0.995$				$q = 0.99$				$q = 0.9845$			
		$x$	$V$	$D_1$	$D_2$	$x$	$V$	$D_1$	$D_2$	$x$	$V$	$D_1$	$D_2$	$x$	$V$	$D_1$	$D_2$
			$km/s$	$10^7 km$	$10^8 km$		$km/s$	$10^7 km$	$10^8 km$		$km/s$	$10^7 km$	$10^8 km$		$km/s$	$10^7 km$	$10^8 km$
1	2.96	0.98300	28.52	0.38749	2.2406	0.99670	28.17	<u>0.07521</u>	2.2718	-	-	-	-	-	-	-	-
	2.95	0.96791	28.84	0.73145	2.2062	0.98115	28.48	0.42965	2.2364	0.99490	28.12	0.11624	2.2677	-	-	-	-
	2.94	0.95327	29.16	1.06515	2.1728	0.96607	28.80	0.77339	2.2020	0.97935	28.44	0.47068	2.2323	0.99455	28.04	0.12421	2.2669
	2.93	0.93900	29.47	1.39042	2.1403	0.95139	29.12	1.10800	2.1685	0.96424	28.76	0.81510	2.1978	0.97891	28.35	0.48071	2.2313
2	2.96	0.94152	28.08	1.33298	2.1461	0.95985	27.57	0.91517	2.1878	0.97957	27.05	0.46567	2.2328	-	-	-	-
	2.95	0.92255	28.52	1.76538	2.1028	0.93971	28.04	1.37424	2.1419	0.95807	27.53	0.95574	2.1838	0.97992	26.95	0.45769	2.2336
	2.94	0.90454	28.96	2.17590	2.0618	0.92071	28.48	1.80732	2.0986	0.93792	27.99	1.41504	2.1378	0.95825	28.05	0.95164	2.1842
	2.93	0.88737	29.38	2.56728	2.0226	0.90269	28.92	2.21807	2.0575	0.91891	28.44	1.84835	2.0945	0.93795	27.90	1.41436	2.1379
3	2.96	0.91532	28.06	1.93018	2.0863	0.93630	27.47	1.45197	2.1342	0.95957	26.84	0.92155	2.1872	0.98875	26.09	2.56425	2.2537
	2.95	0.89429	28.59	2.40954	2.0384	0.91353	28.02	1.97098	2.0823	0.93455	27.43	1.49185	2.1302	0.96036	26.73	0.90354	2.1890
	2.94	0.87465	29.09	2.85722	1.9936	0.89248	28.55	2.45080	2.0343	0.91175	27.98	2.01156	2.0782	0.93506	27.32	1.48023	2.1313
	2.93	0.85619	29.58	3.27799	1.9516	0.87283	29.05	2.89870	1.9895	0.89069	28.51	2.49160	2.0302	0.91204	27.88	2.00495	2.0789
4	2.96	0.89707	28.14	2.34617	2.0447	0.91959	27.49	1.83285	2.0961	0.9451	26.79	1.25138	2.1542	0.9783	25.92	4.94622	2.2299
	2.95	0.87494	28.72	2.85061	1.9943	0.89529	28.12	2.45080	2.0343	0.91785	27.45	1.87251	2.0921	0.9462	26.67	1.22630	2.1567
	2.94	0.8545	29.27	3.31651	1.9477	0.87314	28.68	2.89163	1.9902	0.89353	28.06	2.42686	2.0367	0.91857	27.34	1.85610	2.0937
	2.93	0.83543	29.79	3.75113	1.9042	0.85269	29.23	3.35766	1.9436	0.87137	28.64	2.93187	1.9862	0.89397	27.96	2.41684	2.0377
5	2.96	0.88367	28.25	2.65150	2.0142	0.90711	27.56	2.11732	2.0676	0.93405	26.80	1.50325	2.1290	0.97010	25.85	6.81533	2.2112
	2.95	0.86093	28.85	3.16995	1.9624	0.88190	28.11	2.38675	2.0407	0.90538	27.52	2.15676	2.0637	0.93535	26.68	1.47362	2.1320
	2.94	0.84007	29.43	3.64543	1.9148	0.85915	28.82	3.21052	1.9583	0.88016	28.17	2.73162	2.0062	0.90623	27.40	2.13738	2.0656
	2.93	0.820715	29.98	4.08672	1.8707	0.83829	29.39	3.68601	1.9107	0.85740	28.78	3.25041	1.9543	0.88069	28.06	2.71954	2.0074

Table 5.8: Location, velocity and distance of orbit from both primaries for  $q = 1, 0.995, 0.99, 0.9845$  for Sun–Earth system.

$NL$	$C$	$q = 1$				$q = 0.995$				$q = 0.99$				$q = 0.9845$			
		$x$	$V$	$D_1$	$D_2$	$x$	$V$	$D_1$	$D_2$	$x$	$V$	$D_1$	$D_2$	$x$	$V$	$D_1$	$D_2$
			$km/s$	$10^7 km$	$10^8 km$		$km/s$	$10^7 km$	$10^8 km$		$km/s$	$10^7 km$	$10^8 km$		$km/s$	$10^7 km$	$10^8 km$
1	2.96	0.98305	35.32	0.25352	1.4706	-	-	-	-	-	-	-	-	-	-	-	-
	2.95	0.96795	35.70	0.47942	1.4480	0.98120	35.26	0.28120	1.4678	0.99496	34.88	0.07535	1.4884	-	-	-	-
	2.94	0.95330	36.09	0.69858	1.4261	0.96610	35.64	0.50709	1.4452	0.97940	35.20	0.30813	1.4651	0.99460	34.77	0.08072	1.4879
	2.93	0.93904	36.47	0.91191	1.4048	0.95142	36.03	0.72671	1.4233	0.96425	35.59	0.53477	1.4425	0.97895	35.10	0.31486	1.4645
2	2.96	0.94157	34.74	0.87406	1.4085	0.95990	34.13	0.59985	1.4360	-	-	-	-	-	-	-	-
	2.95	0.92259	35.30	1.15800	1.3801	0.93975	34.69	0.90129	1.4058	0.95813	34.07	0.62633	1.4333	0.98000	33.38	2.99155	1.4660
	2.94	0.90456	35.83	1.42773	1.3532	0.92075	35.24	1.18553	1.3774	0.93796	34.64	0.97803	1.3981	0.95830	33.96	0.62378	1.4336
	2.93	0.88740	36.36	1.68445	1.3275	0.90273	35.78	1.45511	1.3504	0.91895	35.19	1.21246	1.3747	0.93800	34.53	0.92747	1.4032
3	2.96	0.91538	34.72	1.26587	1.3694	0.93635	33.99	0.95215	1.4007	0.95965	33.22	6.03591	1.4356	-	-	-	-
	2.95	0.89434	35.37	1.58062	1.3379	0.91359	34.67	1.29264	1.3667	0.93462	33.94	0.97803	1.3981	0.96045	33.08	5.91623	1.4368
	2.94	0.87469	35.99	1.87459	1.3085	0.89252	35.32	1.60785	1.3352	0.91181	34.62	1.31927	1.3640	0.93513	33.81	0.97041	1.3989
	2.93	0.85623	36.60	2.15075	1.2809	0.87287	35.95	1.90181	1.3058	0.89074	35.27	1.63448	1.3325	0.91210	34.50	1.31493	1.3645
4	2.96	0.89714	34.82	1.53874	1.3421	0.91965	34.02	1.20199	1.3758	0.94520	33.15	8.19763	1.4140	0.97844	32.11	3.22492	1.4637
	2.95	0.87499	35.53	1.87010	1.3089	0.89535	34.78	1.56551	1.3394	0.91793	33.97	1.22772	1.3732	0.94630	33.01	8.03307	1.4156
	2.94	0.85454	36.21	2.17603	1.2783	0.87320	35.49	1.89688	1.3063	0.89359	34.73	1.59184	1.3368	0.91865	33.83	1.21695	1.3743
	2.93	0.83547	36.86	2.46132	1.2498	0.85274	36.16	2.20296	1.2757	0.87142	35.44	1.92351	1.3036	0.89403	34.59	1.58526	1.3374
5	2.96	0.88373	34.95	1.73935	1.3220	0.90719	34.10	1.38839	1.3571	0.93415	33.17	9.85071	1.3974	0.97030	32.01	4.44267	1.4515
	2.95	0.86099	35.70	2.08089	1.2879	0.88195	34.71	1.41427	1.3545	0.90546	34.05	1.41427	1.3545	0.93547	33.01	9.65323	1.3994
	2.94	0.84012	36.41	2.39175	1.2568	0.85920	35.65	2.10632	1.2853	0.88022	34.85	1.79186	1.3168	0.90630	33.91	1.40170	1.3558
	2.93	0.82075	37.09	2.68153	1.2278	0.83833	36.36	2.41853	1.2541	0.85745	35.60	2.13250	1.2827	0.88075	34.72	1.78393	1.3176

## 5.3 Conclusion

We have investigated the effect of solar radiation pressure on the position, shape and size of closed periodic orbit with loops varying from 1 to 5 for Sun–Mars and Sun–Earth systems, respectively. A noticeable difference observed in both the systems is that for  $C = 2.96$ ,  $q = 0.995$ , single–loop periodic orbit, for  $C = 2.96$ ,  $q = 0.99$ , two–loops orbit, and for  $C = 2.96$ ,  $q = 0.9845$ , three–loops periodic orbit does not exist for Sun–Earth system whereas it exists for Sun–Mars system.

The distance of closest approach of the secondary body from the smaller primary decreases with increase in perturbation due to solar radiation pressure from 1 to 0.9845 and distance between smaller primary and secondary body increases as number of loops increases for a given  $C$  and  $q$ . It is found that eccentricity decreases as the number of loops increases. For a given number of loops, eccentricity decreases as solar radiation pressure increases from 1 to 0.9845. Thus, the present analysis of the two systems–Sun–Mars and Sun–Earth systems–using PSS technique reveals that  $q$  and  $C$  has substantial effect on the position, shape and size of the orbit.

It can be observed that for given solar radiation pressure and given number of loops, as Jacobi constant decreases, initial velocity of secondary body (spacecraft) and distance of spacecraft from second primary increase and distance of it from first primary body decreases. For given Jacobi constant and given number of loops, as perturbation due to solar radiation pressure increases from 1 to 0.9845, initial velocity decreases and distance of spacecraft from second primary decreases. So, distance of it from first primary increases. Thus, the effect of  $C$  and  $q$  is opposite in nature. For given value of solar radiation pressure  $q$  and Jacobi constant  $C$ , as number of loops increases, distance of spacecraft from second primary increases and distance of it from first primary decreases. It is further observed that for Sun–Mars system, single–loop orbit for  $q = 0.995$  and  $C = 2.96$  is closest to Mars and this distance is  $7.521 \times 10^5$  kms, whereas for Sun–Earth system, single–loop orbit for  $q = 0.99$  and  $C = 2.95$  is closest to Earth and this distance is  $7.535 \times 10^5$  kms. Therefore, these orbits can be used for designing low–energy space mission.

Stability analysis of the family of orbits indicates that these orbits have smaller stability region in comparison to  $f$  family orbit studied in chapter 3. So, these orbits can be used as a transfer trajectory as less amount of fuel required for transferring

---

of satellite from one orbit to another orbit. For each pair  $(q, C)$ , there exists two separatrices where the stability of periodic orbits is zero.